

# Velocity Map Imaging VUV Angle-Resolved Photoelectron Spectroscopy of Isolated Silver Sulfide Nanoparticles

Danijela Danilović<sup>1</sup>, Dušan K. Božanić<sup>1,\*</sup>, Gustavo A. Garcia<sup>2</sup>, Laurent Nahon<sup>2</sup>, Una Stamenović<sup>1</sup>, Vesna V. Vodnik<sup>1</sup>, and Vladimir Djoković<sup>1,\*</sup>

<sup>1</sup>Department of Radiation Chemistry and Physics, "Vinča" Institute of Nuclear Sciences - National Institute of the Republic of Serbia, University of Belgrade, P.O. Box 522, 11001 Belgrade, Serbia

<sup>2</sup>Synchrotron SOLEIL, l'Orme des Merisiers, St. Aubin, BP48, 91192 Gif sur Yvette Cedex, France

Corresponding authors: \*D.K.B. [bozanic@vin.bg.ac.rs](mailto:bozanic@vin.bg.ac.rs); V.Dj. [djokovic@vin.bg.ac.rs](mailto:djokovic@vin.bg.ac.rs)

## Abstract

The angle-resolved photoelectron spectroscopy of isolated silver sulfide nanoparticles was carried out by using velocity map imaging technique at the DESIRS beamline of SOLEIL synchrotron facility. The reported spectroscopy results were obtained after interaction of the synchrotron radiation with a polydisperse aerosol produced from aqueous dispersion of silver sulfide particles, approximately 16 nm in diameter. The photoelectron and UV-Vis-NIR absorption spectra were used to estimate the maximum energy of the valence- and the minimum energy of the conduction-band of the nanoparticles. With respect to the vacuum level, the obtained values were found to be  $5.5 \pm 0.1$  eV and  $4.5 \pm 0.1$  eV for the valence band maximum and conduction band minimum, respectively. The dependence of the asymmetry parameter on the electron energy along the silver sulfide valence band showed an onset of inelastic scattering at  $\sim 1$  eV electron kinetic energy.

**Keywords:** silver-sulfide nanoparticles; valence band structure; photoelectron spectroscopy; vacuum ultraviolet radiation

## Introduction

Photoelectron spectroscopy of nanosystems isolated in the gas-phase is an essential method for the assessment of electronic structure of nanoparticles without the influence of a substrate [1, 2]. The method is based on the interaction of free-flying nanoparticles, focused into an aerosol beam few hundred micrometers in diameter under high vacuum conditions, with vacuum ultraviolet (VUV) [3, 4] or soft x-ray [5, 6] electromagnetic radiation. The interaction results in series of processes which can be well analyzed by using velocity map imaging (VMI), a technique which allows for simultaneous measurement of kinetic energy and angular ( $4\pi$  sr) distributions of low-kinetic energy photoelectrons [7, 8]. This technique also enables a facile differentiation between the electrons originating from the nanoparticles and gas-phase molecules, due to asymmetry of the signals with respect to the direction of the propagation of the incident radiation, because of so-called shadowing effect [9]. The removal of the contributions of the gas-phase molecules to the electron images was reported for the experiments conducted in photoelectron-photoion coincidence (PEPICO) detection scheme [4, 5]. So far, several nanosystems were investigated by VUV velocity map imaging photoemission spectroscopy (VUV VMI-

PES). These include NaCl particles [9], gold nanoparticles [4], methylammonium lead bromide perovskite nanocrystals [5], charge transfer complexes based on colloidal TiO<sub>2</sub> nanoparticles [10], and chiral nanosystems produced from serine aqueous solutions [11]. In this study, we report on the electron energy and angular distributions of the photoelectrons emitted from isolated silver sulfide nanoparticles (Ag<sub>2</sub>S NP).

Silver sulfide is a narrow band gap semiconductor (~1 eV) that shows great promise for application in photovoltaic cells and in radiation detectors that operate in the near infrared domain [12]. On the other hand, due to their size-dependent absorption and fluorescence in the second near-infrared optical window (NIR-II), silver sulfide nanoparticles became important nanostructured probes for fluorescence and photoacoustic imaging of cells and tissues [13, 14]. Nanostructured Ag<sub>2</sub>S layers were also used as NIR absorbers to increase the efficiency of solar cells [15] or as sensitizers to TiO<sub>2</sub> for photocatalytic hydrogen generation [16, 17]. In these applications, the efficiency of electronic processes of Ag<sub>2</sub>S NPs does not depend on the energy of the band gap only but also on their valence band structure, i.e. the alignment of HOMO/LUMO levels of Ag<sub>2</sub>S with the valence levels of other components in the investigated systems. Photoelectron spectroscopy is the typical method for determination of the energy levels in multicomponent solid systems. However, conventional photoelectron spectroscopy techniques measure the energies of the valence bands relative to the Fermi level. Information on the ionization energies of Ag<sub>2</sub>S referenced to the vacuum level is still very limited [18], whereas, to the best of our knowledge, there is no information in the literature on the isolated Ag<sub>2</sub>S NP. Therefore, in the present study, we report on the valence band structure of Ag<sub>2</sub>S NP by synchrotron radiation VUV VMI-PES.

## **Experimental methods**

### *Materials*

Silver nitrate (AgNO<sub>3</sub>), trisodium citrate (Na-cit), sodium borohydride (NaBH<sub>4</sub>), and thioacetamide (TAA) were obtained from Sigma Aldrich and used as received. High purity water (18.2 MΩ cm<sup>-1</sup>) was used in all synthetic procedures).

### *Synthesis of Ag<sub>2</sub>S nanoparticles*

Batch aqueous solutions of AgNO<sub>3</sub> (50 mM), Na-cit (38.8 mM) and TAA (0.1 M) were prepared immediately before the synthesis. To prepare Ag<sub>2</sub>S NP, 122 μl of AgNO<sub>3</sub> batch solution was mixed with 5 ml of water followed by addition of 45 ml of solution containing 0.9 mg NaBH<sub>4</sub> and 2.32 ml of Na-cit batch solution under vigorous stirring. The solution immediately turned yellow indicating the formation of silver nanoparticles. The solution was brought to boil under constant stirring and, subsequently, 30.5 μl of TAA batch solution was added and stirred for additional 10 minutes.

### *Characterization of Ag<sub>2</sub>S nanoparticles*

Transmission electron microscopy (TEM) was carried out on a JEOL JEM-1400 instrument operating at 120 kV. The size distribution of Ag<sub>2</sub>S nanoparticles was measured by dynamic light scattering (DLS) using a Nanotrak ULTRA (Microtrac) instrument. The UV-Vis-NIR absorption spectrum of Ag<sub>2</sub>S hydrocolloid was measured by a Shimadzu UV-2600 (Shimadzu Corporation, Japan) spectrophotometer in a 250-1300 nm range.

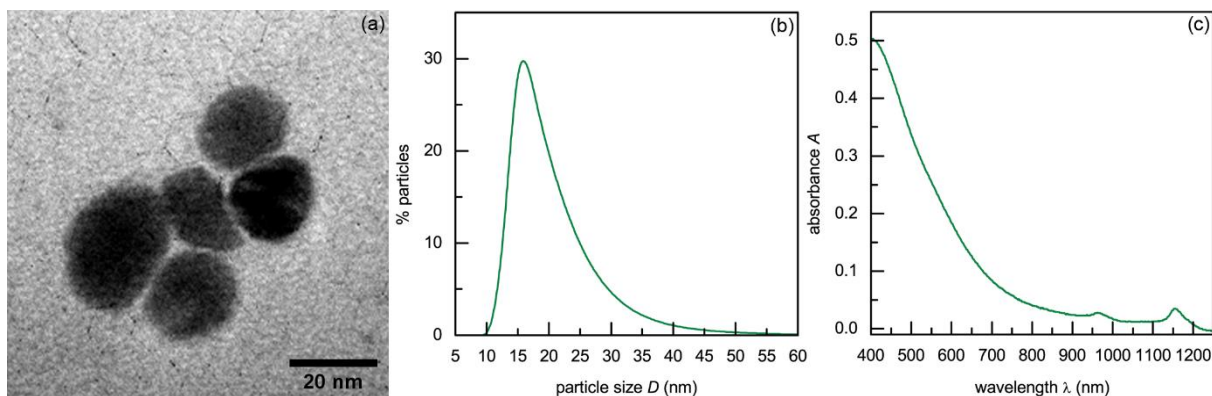
### *VUV VMI-PES of isolated Ag<sub>2</sub>S nanoparticles*

The VUV VMI-PES experiments were performed on the SAPHIRS endstation [19] located on one of the monochromatized branches of the variable polarization undulator-based VUV beamline DESIRS [20] at Synchrotron SOLEIL. Details of the experimental procedures for conducting VUV VMI-PES measurements

are given in Ref. [4]. Briefly, Ag<sub>2</sub>S aerosols were produced by atomization of the Ag<sub>2</sub>S hydrocolloid using a TSI 3076 constant output atomizer operating with 2.5 bars of argon as carrier gas. The aerosols were dried by a 2 m long diffusion drier filled with silica gel and introduced via a 200 μm limiting orifice into the aerodynamic lens. The aerodynamic lens focused the particle beam, via differential pumping stages, into the ionization chamber at  $\sim 10^{-8}$  mbar base pressure. The particle beam was crossed by a beam of circularly polarized synchrotron radiation ( $h\nu=8$  eV and 11 eV, flux  $\sim 10^{12}$  photons/sec). Photoelectron images were detected by the velocity map imaging spectrometer [21]. The kinetic energy distribution, i.e. the photoelectron emission spectrum (PES), and the asymmetry and anisotropy of the angular distribution as a function of kinetic energy are obtained from the inverted photoelectron images using a modified version of the pBasex algorithm [4].

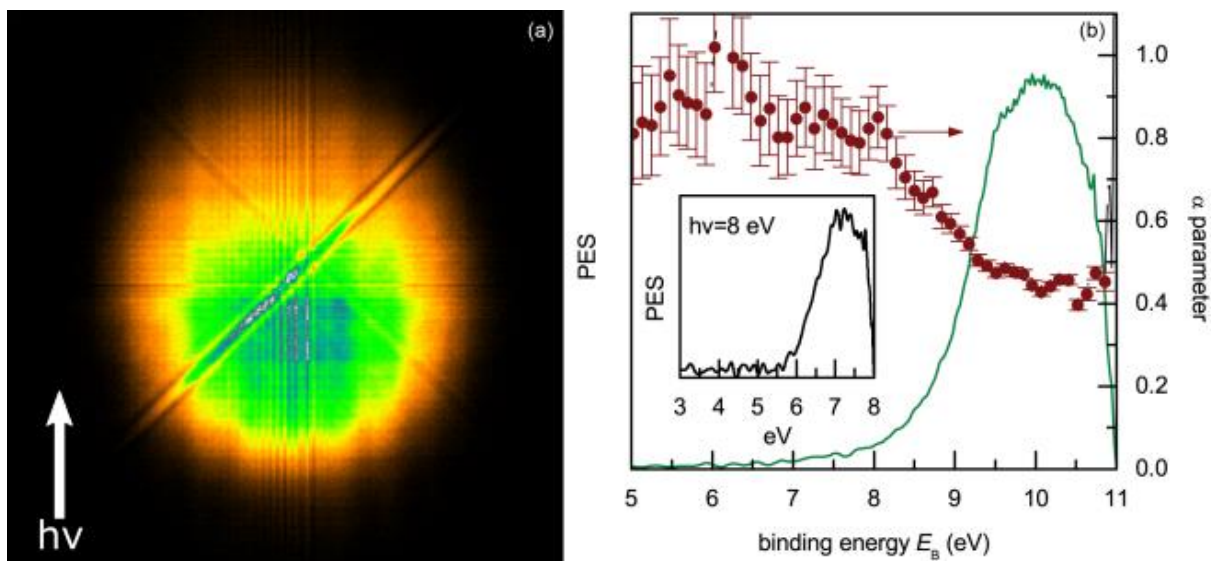
## Results and Discussion

Figure 1 shows the results of the characterization of as prepared Ag<sub>2</sub>S NP. The size and morphology of the nanoparticles were investigated by TEM (Figure 1a). The particles were ellipsoidal in shape and approximately 20 nm in size. The DLS measurements (Figure 1b) showed log-normal distribution of particle sizes with an average value of the hydrodynamic diameter of 16 nm. The UV-Vis-NIR spectrum of the Ag<sub>2</sub>S hydrocolloid showed typical monotonically decreasing behavior in the visible region [22, 23], and the onset of the absorption at 1240 nm ( $E_g=1$  eV), which originates from valence to conduction band transitions. In addition, weak absorption bands at  $\sim 970$  nm and  $\sim 1100$  nm can be observed, which probably originate from the light absorption of much smaller Ag<sub>2</sub>S NPs. Unfortunately, we were not able to unambiguously prove the presence of smaller particles by TEM due to the low acceleration voltage of the instrument.



**Figure 1.** Characterization of Ag<sub>2</sub>S NP: (a) TEM image, (b) particle size distribution measured by DLS, and (c) UV-vis absorption spectra of Ag<sub>2</sub>S hydrocolloid.

The results of the VUV VMI-PES of Ag<sub>2</sub>S nanoparticles recorded at  $h\nu=11$  eV photon energy are presented in Figure 2. The Ag<sub>2</sub>S particle beam consisted of  $D_a \sim 100$  nm in size aerosol particles comprised of individual Ag<sub>2</sub>S primary nanoparticles, which was confirmed by complementary scanning mobility particle size and scanning electron microscopy measurements (not shown). As it was demonstrated in our previous study [4], due to the small size of the electron scattering length ( $\lambda_e=2-3$  nm) in comparison to the photon attenuation depth ( $\Lambda \sim 20$  nm) in the VUV domain, the size of the aerosol particles does not significantly affect the photoelectron energy distribution. However, since in this nanosystem  $\Lambda < D_a$ , more photoelectrons should be emitted from the particles on the directly irradiated side, leading to a forward/backward asymmetry in the photoelectron angular distribution [9]. Typical background-corrected electron image (Figure 2a) shows a clear asymmetry in the direction of the photon beam propagation, thus confirming that the synchrotron radiation was probing the aerosol particles [9, 4, 10].



**Figure 2.** (a) Background-corrected electron image. The arrow indicates the direction of the propagation of the synchrotron radiation. (b) Photoemission spectrum (green line) and asymmetry parameter  $\alpha$  dependence on the binding energy for  $\text{Ag}_2\text{S}$  NP recorded at  $h\nu=11$  eV. Inset: Photoemission spectrum of  $\text{Ag}_2\text{S}$  NP recorded at  $h\nu=8$  eV. The binding energies in (b) are referenced to the vacuum level.

The photoemission spectrum and the dependence of the asymmetry parameter  $\alpha$  on the electron binding energy are presented in Figure 2b. The PES of  $\text{Ag}_2\text{S}$  NP shows a broad band that originates from hybridized Ag 4d and S 2p states [24]. The ionization energy of the  $\text{Ag}_2\text{S}$  NP was investigated by using 8 eV photon energy (inset to Figure 2), which enables a high precision measurement. The onset of the ionization, corresponding to the valence band maximum, was found to be  $IE=5.5\pm 0.1$  eV, which is in accordance with the previously reported value of 5.42 eV [18]. By comparing the experimental IE value with the band gap obtained from optical absorption (Figure 1c), we can estimate the energy of the minimum of the conduction band at  $4.5\pm 0.1$  eV below the vacuum level. The asymmetry parameter  $\alpha$ , plotted in Figure 2b and defined as a ratio between the number of electrons emitted in forward and backward directions [9] for a given electron energy, shows nearly constant values between 10 eV and 11 eV binding energy (0 - 1 eV kinetic energy). There is an increase in symmetry towards lower binding energies. This effect may occur as a consequence of a decrease in the total photoelectron count as the electron energy approaches the top of the valence band (5.5 eV) or due to emergence of the inelastic scattering processes in  $\text{Ag}_2\text{S}$  NP for of the photoelectron kinetic energies higher than  $\sim 1$  eV [4].

## Conclusion

In summary, synchrotron radiation VUV VMI-PES study of isolated silver sulfide particles produced by atomization of hydrocolloid containing  $\text{Ag}_2\text{S}$  NP 16 nm in size was performed. The ionization energy of  $\text{Ag}_2\text{S}$  NP was experimentally determined to be  $5.5\pm 0.1$  eV with respect to the vacuum level. This value allowed for the estimation of energy of the minimum of the conduction band at  $4.5\pm 0.1$  eV, using the value for the band gap of 1 eV obtained from the UV-Vis-NIR absorption spectroscopy. The angular distribution of the photoelectrons suggested that the inelastic processes take place in  $\text{Ag}_2\text{S}$  for the photoelectrons with the kinetic energies higher than 1 eV. The results presented could be of significance for the future studies of charge transfer processes in hybrid nanostructures containing  $\text{Ag}_2\text{S}$  NP, which can lead to more efficient nanoscale systems used for imaging of tissues, hydrogen production, and/or for light-absorbing materials in solar cells.

## Acknowledgments

The VUV VMI-PES experiments on isolated Ag<sub>2</sub>S NP were performed at the DESIRS beamline at Synchrotron SOLEIL as a part of the research project no. 20180566. The authors acknowledge the support of the entire staff of Synchrotron SOLEIL for smooth operation during the beamtime. The authors are also grateful to Ministry of Education, Science and Technological Development of the Republic of Serbia for financial support.

## Statements and Declarations

The authors have no competing interests to declare that are relevant to the content of this article.

## References

- <sup>1</sup> K. R. Wilson, H. Bluhm, and M. Ahmed, *Aerosol Photoemission*, in *Fundamentals and Applications in Aerosol Spectroscopy*, ed. by R. Signorell and J. P. Reid, CRC Press 2011.
- <sup>2</sup> L. Ban, B. L. Yoder, and R. Signorell, *Annu. Rev. Phys. Chem.* **71**, 315 (2020).
- <sup>3</sup> F. Gaie-Levrel, G. A. Garcia, M. Schwell, and L. Nahon, *Phys. Chem. Chem. Phys.* **13**, 7024 (2011).
- <sup>4</sup> D.K. Bozanic, G.A.Garcia, O. Sublemontier, J. Pajovic, V. Dokovic, and L. Nahon, *J. Phys. Chem. C* **124**, 24500 (2020).
- <sup>5</sup> A. R. Milosavljević, D. K. Božanić, S. Sadhu, N. Vukmirović, R. Dojčilović, P. Sapkota, W. Huang, J. Bozek, C. Nicolas, L. Nahon, and S. Ptasinska, *J. Phys. Chem. Lett.* **9**, 3604 (2018).
- <sup>6</sup> D. Danilovic, D. K. Bozanic, R. Dojcilovic, N. Vukmirovic, P. Sapkota, I. Vukasinovic, V. Djokovic, J. Bozek, C. Nicolas, S. Ptasinska, and A. Milosavljevic, *J. Phys. Chem. C* **124**, 23930 (2020).
- <sup>7</sup> A.T.J.B. Eppink, D.H. Parker, *Rev. Sci. Instrum.* **68**, 3477 (1997).
- <sup>8</sup> A. G. Suits and R. E. Continetti, *Imaging in chemical dynamics* (American Chemical Society, Washington D.C., 2000).
- <sup>9</sup> K. R. Wilson, S. Zou, J. Shu, E. Ruhl, S. R. Leone, G. C. Schatz, and M. Ahmed, *Nano Letters* **7**, 2014 (2007)
- <sup>10</sup> D. K. Božanić, G. A. Garcia, L. Nahon, D. Sredojević, V. Lazić, I. Vukoje, S. P. Ahrenkiel, V. Djoković, Ž. Šljivančanin, J.M. Nedeljković, *J. Phys. Chem. C* **123**, 29057 (2019)
- <sup>11</sup> S. Hartweg, G.A. Garcia, D. K. Bozanic, and L. Nahon, *J. Phys. Chem. Lett.* **12**, 2385 (2021).
- <sup>12</sup> K. Akamatsu, S. Takei, M. Mizuhata, A. Kajinami, S. Deki, S. Takeoka, M. Fujii, S. Hayashi, K. Yamamoto, *Thin Solid Films* **55**, 359 (2000).
- <sup>13</sup> D-H. Zhao, J. Yang, R-X. Xia, M-H. Yao, R-M. Jin, Y-D. Zhao, and B. Liu, *Chem. Comm.* **54**, 527 (2018).
- <sup>14</sup> X. Zhang, W. Wang, L. Su, X. Ge, J. Ye, C. Zhao, Y. He, H. Yang, J. Song, and H. Duan, *Nano Lett.* **21**, 2625 (2021).
- <sup>15</sup> Y. Cao, M. Bernechea, A. Maclachlan, V. Zardetto, M. Creatore, A.A. Haque, and G. Konstantatos, *Chem. Mater.* **27**, 3700 (2015).
- <sup>16</sup> K. Nagasuna, T. Akita, M. Fujishima, and H. Tada, *Langmuir* **27**, 7294 (2011).
- <sup>17</sup> M. Gao, L. Zhu, C. K. N. Peh, G.W. Ho, *Procedia Eng.* **215**, 188 (2017).
- <sup>18</sup> N. Zhang, M. Li, C. F. Tan, C. K. N. Peh, T. C. Sum, G.W. Ho, *J. Mater. Chem. A* **5**, 21570 (2017).
- <sup>19</sup> X. Tang, G. A. Garcia, J.-F. Gil, and L. Nahon, *Rev. Sci. Instrum.* **86**, 123108 (2015).
- <sup>20</sup> L. Nahon, N. de Oliveira, G. A. Garcia, J.-F. Gil, B. Pilette, O. Marcouillé, B. Lagarde and F. Polack, *J. Synchrotron Rad.* **19**, 508 (2012).
- <sup>21</sup> G. A. Garcia, B. K. Cunha de Miranda, M. Tia, S. Daly, and L. Nahon, *Review of Scientific Instruments* **84**, 053112 (2013).
- <sup>22</sup> V. Djokovic, R. Krsmanovic, D.K. Bozanic, M. McPherson, G. Van tendeloo, P. Sreekumari Nair, M.K. Georges, and T. Radhakrishnan, *Coll. Surf. B* **73**, 30 (2009).
- <sup>23</sup> L.V. Trandafilovic, V. Djokovic, N. Bibic, M.K. Georges, and T. Radhakrishnan, *Mater. Lett.* **64**, 1123 (2010).
- <sup>24</sup> S. Kashida, N. Watanabe, T. Hasegawa, H. Iida, M. Mori, and S. Savrasov, *Solid State Ionics* **158**, 157 (2003).